

MITOCHONDRIAL OXYGEN AFFINITY, RESPIRATORY FLUX CONTROL AND EXCESS CAPACITY OF CYTOCHROME *c* OXIDASE

ERICH GNAIGER*, BARBARA LASSNIG, ANDREY KUZNETSOV, GUNDE RIEGER
 AND RAIMUND MARGREITER

Department of Transplant Surgery, D. Swarovski Research Laboratory, University Hospital Innsbruck, Anichstraße 35, A-6020 Innsbruck, Austria

*e-mail: erich.gnaiger@uibk.ac.at

Accepted 9 February; published on WWW 24 March 1998

Summary

The oxygen affinity of the enzyme system involved in mitochondrial respiration indicates, in relation to intracellular oxygen levels and interpreted with the aid of flux control analysis, a significant role of oxygen supply in limiting maximum exercise. This implies that the flux control coefficient of mitochondria is not excessively high, based on a capacity of mitochondrial oxygen consumption that is slightly higher than the capacity for oxygen supply through the respiratory cascade. Close matching of the capacities and distribution of flux control is consistent with the concept of symmorphosis. Within the respiratory chain, however, the large excess capacity of cytochrome *c* oxidase, COX, appears to be inconsistent with the economic design of the respiratory cascade. To address this apparent discrepancy, we used three model systems: cultured endothelial cells and mitochondria isolated from heart and liver. Intracellular oxygen gradients increase with oxygen flux, explaining part of the observed decrease in oxygen affinity with increasing metabolic rate in cells. In addition, mitochondrial oxygen affinities decrease from the resting

to the active state. The oxygen affinity in the active ADP-stimulated state is higher in mitochondria from heart than in those from liver, in direct relationship to the higher excess capacity of COX in heart. This yields, in turn, a lower turnover rate of COX even at maximum flux through the respiratory chain, which is necessary to prevent a large decrease in oxygen affinity in the active state. Up-regulation of oxygen affinity provides a functional explanation of the excess capacity of COX. The concept of symmorphosis, a matching of capacities in the respiratory cascade, is therefore complemented by 'synkinetic' considerations on optimum enzyme ratios in the respiratory chain. Accordingly, enzymatic capacities are matched in terms of optimum ratios, rather than equal levels, to meet the specific kinetic and thermodynamic demands set by the low-oxygen environment in the cell.

Key words: oxygen flux, catalytic efficiency, hypoxia, respiratory cascade, respiratory chain, flux control analysis, endothelial cell, liver, heart, mitochondria.

Respiratory cascade to respiratory chain

The mitochondrial respiratory chain fulfils the kinetically and thermodynamically complex tasks of (1) catalysing a high electron flux to oxygen in active metabolic states and (2) pumping protons at high efficiency as a basis for intense aerobic ATP production. Moreover, these functions must be (3) performed at low intracellular oxygen pressure, which requires a high affinity for oxygen (Babcock and Wikström, 1992).

Oxygen in the environment is globally stable when measured at the scale of generations, but varies locally and may become limiting under diverse environmental and physiological conditions. Respiration of all organisms is a function of the partial pressure of oxygen, P_{O_2} , below a critical environmental oxygen pressure, depending on the structural and functional capacities and regulatory mechanisms at all steps of the respiratory cascade (Fig. 1). The form of the oxygen-dependence varies among species and may be

complex, yet a surprisingly simple hyperbolic equation describes the flux/pressure relationship in some cases (Gnaiger, 1993a). The rectangular hyperbolic equation with an intercept through the origin:

$$J_{O_2} = \frac{J_{\max} \times P_{O_2}}{P_{50} + P_{O_2}}, \quad (1)$$

where J_{O_2} is oxygen flux, is characterised by two parameters, P_{50} , the oxygen partial pressure at which respiratory flux is 50 % of maximum, and J_{\max} , the maximum oxygen flux, at saturating oxygen levels. J_{\max} is a function of metabolic state. At maximum aerobic power, the corresponding J_{\max} may be estimated approximately at a plateau of non-limiting, possibly hyperoxic, oxygen pressures greater than 20 kPa. Differences in J_{O_2} of a few per cent are usually within experimental error but might be important indications that oxygen saturation is

nearly but not fully reached. Accurate determination of J_{\max} , therefore, requires statistical evaluation over the entire range of oxygen concentration. This is not a simple task in athletes or animal models at maximum levels of exercise (Chance *et al.* 1985; Wagner, 1996).

When studying the respiration of isolated cells, the major pathway for oxygen from the environment along the respiratory cascade (Weibel, 1984) is removed (Fig. 1), and the relevant P_{O_2} range is reduced from more than 20 to 1 kPa. In tumour vessels, for instance, *in vivo* P_{O_2} values as low as 0.7 kPa are not hypoxic (Helmlinger *et al.* 1997). Under the simpler conditions for oxygen transport from extracellular P_{O_2} to the terminal oxidase, a hyperbolic oxygen-dependence (equation 1) is more generally observed (for a review, see Gnaiger *et al.* 1995), despite the remaining complexities of intracellular oxygen gradients and heterogeneities of lipid and aqueous phases and mitochondrial clusters (Fig. 2).

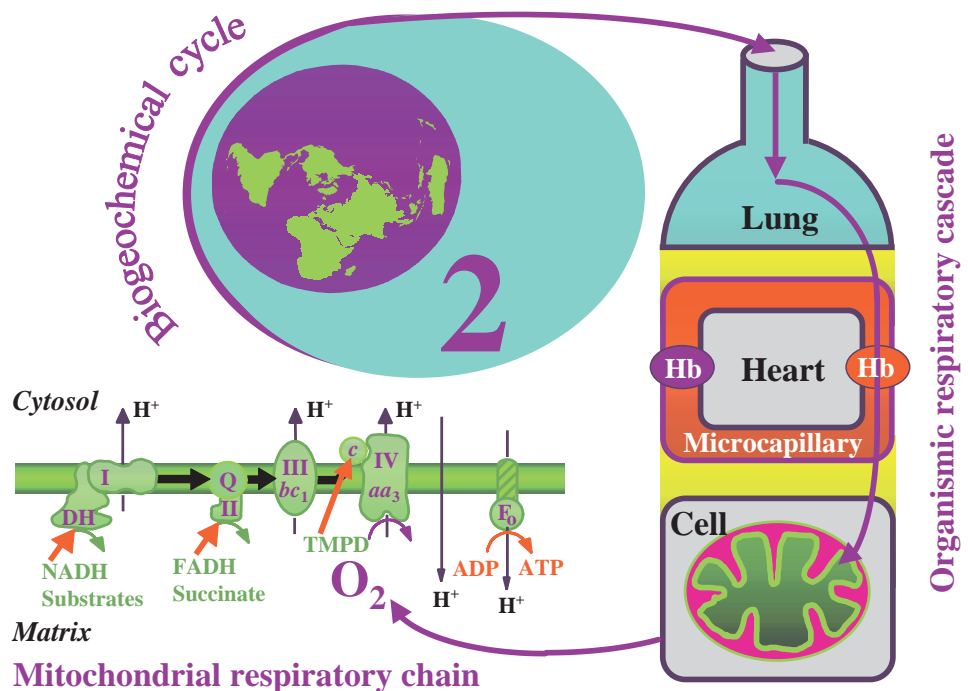
A further shortcut for oxygen delivery to the actual site of conversion of oxygen to water is afforded by the study of isolated mitochondria. A myoglobin saturation of approximately 50% is typical for the volume-averaged intracellular oxygen pressure in heart and skeletal muscle, corresponding to 0.3 kPa (2 mmHg, $3 \mu\text{mol l}^{-1}$; Wittenberg and Wittenberg, 1989; Wagner, 1996). In the physiologically relevant intracellular P_{O_2} range below 1 kPa, respiration can again be described by a hyperbolic function. Measurements

with mitochondria at much higher oxygen levels appear to ignore this physiological background of the respiratory cascade (Gnaiger *et al.* 1995).

Biochemists frequently refer to the P_{50} as the apparent Michaelis–Menten constant for oxygen, K_m' . However, even this mitochondrial compartment at the end of the respiratory cascade is a highly complex metabolic network, harbouring the multienzyme system known as the mitochondrial respiratory chain (Fig. 1). Since the oxygen-dependence of organismic respiration is sensitive to each component of the respiratory cascade, so is the mitochondrial P_{50} potentially a function of each element in the respiratory chain, in contrast to the terminological implications of a K_m' 'constant'.

In the present work, we address four aspects of mitochondrial oxygen kinetics, aiming at an integration of physiological and bioenergetic perspectives. (1) The current status of mitochondrial oxygen kinetics is reviewed in terms of experimentally determined P_{50} values. (2) P_{50} increases with the rate of oxidative phosphorylation and is a function of metabolic state (coupled *versus* uncoupled respiration). (3) Oxygen affinity, i.e. the reciprocal value of P_{50} , provides insufficient information on oxygen kinetics when J_{\max} is a function of oxygen-independent parameters, such as ADP concentration. Under these conditions, the apparent catalytic efficiency, J_{\max}/P_{50} , is physiologically relevant to describe respiratory control by low oxygen levels. While affinity

Fig. 1. Oxygen flux from the environment, characterised by the biogeochemical cycle, through the organismic respiratory cascade (Weibel, 1984) to the mitochondrial respiratory chain. Mitochondrial electron transport is shown in the inner mitochondrial membrane, with redox proteins and proton pumps (complexes I–IV). Horizontal arrows show electron flow, finally reducing O_2 to water (complex IV, cytochrome *c* oxidase, COX) as measured by respirometry. Vertical arrows show transmembrane proton flows. Electrons from NADH enter the respiratory chain at complex I (NADH–CoQ reductase), which is inhibited by rotenone. Succinate enters at complex II (succinate–CoQ reductase). In general, electron transfer to ubiquinol (Q) is effected by parallel pathways through multiple dehydrogenases (Trumpower and Gennis, 1994). After blocking electron flow at complex III (CoQH₂–*c* reductase) with antimycin A, *N,N,N',N'*-tetramethyl-*p*-phenylenediamine dihydrochloride (TMPD) is added as an artificial electron donor to cytochrome *c* to study the activity of COX. Proton pumping generates a proton-motive force across the inner mitochondrial membrane which inhibits O_2 flux at rest in the absence of ADP. Maximum stimulation by ADP and inorganic phosphate leads to a decline in the proton-motive force and maximum flux at reduced thermodynamic efficiency of proton translocation. The uncoupler carbonyl cyanide *p*-trifluoromethoxyphenylhydrazone (FCCP) reduces the membrane potential further by short-circuiting proton flow and eliminating adenylate control. Mitochondrial oxygen kinetics is studied under these different metabolic states and rates. *aa*₃, *bc*₁, *c*, cytochromes; DH, NADH dehydrogenase complex; *F*₀, ATP synthetase; Hb, haemoglobin; CoQ, coenzyme Q.



with mitochondria at much higher oxygen levels appear to ignore this physiological background of the respiratory cascade (Gnaiger *et al.* 1995).

Biochemists frequently refer to the P_{50} as the apparent Michaelis–Menten constant for oxygen, K_m' . However, even this mitochondrial compartment at the end of the respiratory cascade is a highly complex metabolic network, harbouring the multienzyme system known as the mitochondrial respiratory chain (Fig. 1). Since the oxygen-dependence of organismic respiration is sensitive to each component of the respiratory cascade, so is the mitochondrial P_{50} potentially a function of each element in the respiratory chain, in contrast to the terminological implications of a K_m' 'constant'.

In the present work, we address four aspects of mitochondrial oxygen kinetics, aiming at an integration of physiological and bioenergetic perspectives. (1) The current status of mitochondrial oxygen kinetics is reviewed in terms of experimentally determined P_{50} values. (2) P_{50} increases with the rate of oxidative phosphorylation and is a function of metabolic state (coupled *versus* uncoupled respiration). (3) Oxygen affinity, i.e. the reciprocal value of P_{50} , provides insufficient information on oxygen kinetics when J_{\max} is a function of oxygen-independent parameters, such as ADP concentration. Under these conditions, the apparent catalytic efficiency, J_{\max}/P_{50} , is physiologically relevant to describe respiratory control by low oxygen levels. While affinity

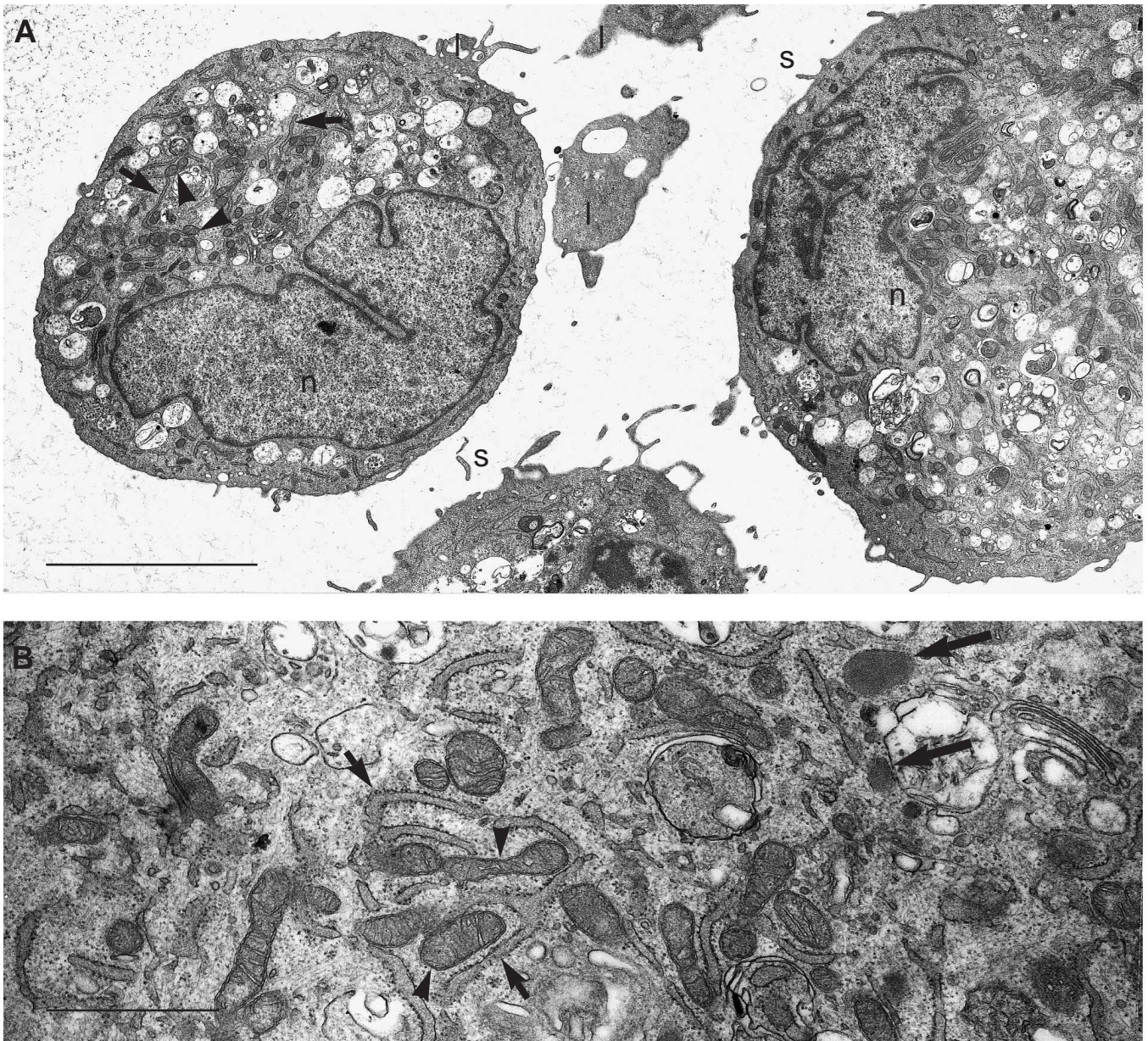


Fig. 2. Ultrastructure of human umbilical vein endothelial cells (HUVECs) suspended in endothelial culture medium. (A) The spherical cells show large lobate nuclei (n) and a correspondingly uneven distribution of mitochondria (arrowheads). Cell extensions (lamellipodia, l) are retracted to varying degrees and some microspikes (s) are always present. Extensions frequently contain rough endoplasmic reticulum cisternae (small arrows) and occasionally contain mitochondria. Scale bar, 5 μm . (B) Elongate mitochondria (arrowheads) with regularly arranged lamelliform cristae and medium-dense matrix. Mitochondria are closely associated with the network of rough endoplasmic reticulum (small arrows). The numerous Weibel–Palade bodies (large arrows) are of similar size to mitochondria. Scale bar, 1 μm . Cells were fixed by injecting glutaraldehyde into a sample taken from the stirred oxygraph chamber (2.5 % final concentration, for 90 min at 4 °C). After centrifugation, the pellet was washed and resuspended in agar. The hardened agar pellet was cut into small pieces for post-fixation in 2 % OsO_4 (0.05 mol l^{-1} sodium cacodylate buffer, 60 min) and serial dehydration. Thin sections were stained with saturated aqueous uranyl acetate and lead citrate and examined using a Zeiss 902 transmission electron microscope.

decreases, the apparent catalytic efficiency increases from the resting to the active state and increases in general as the thermodynamic efficiency of energy conversion decreases. This analysis sets the stage for (4) a discussion of the oxygen kinetics of the mitochondrial respiratory chain in relation to the organismic respiratory cascade (Fig. 1), with reference to the

concept of symmorphosis (Weibel *et al.* 1991). The excess capacity of cytochrome *c* oxidase (COX) relative to the capacity of the integrated respiratory chain and respiratory cascade is functionally explained as a regulatory mechanism for maintaining a high oxygen affinity by a COX turnover rate that is low even at maximum aerobic performance.

Oxygen affinity and metabolic state/rate

The conflicting views on the role of oxygen in respiratory control are mainly due to uncertainties about intracellular gradients and levels of oxygen in the mitochondrial microenvironment and to the difficulties of making respiratory measurements at the corresponding low oxygen concentrations (Gnaiger *et al.* 1995). Is intracellular P_{O_2} limiting under physiological conditions? Negative answers to this important question refer to a value for P_{50} for mitochondrial respiration of 0.005 kPa, which is nearly 100 times below intracellular oxygen levels (Cole *et al.* 1982; Gayeski and Honig, 1991; Wittenberg and Wittenberg, 1985), whereas an affirmation relates to more recent data on P_{50} values that are less than one-tenth of intracellular P_{O_2} (Wilson *et al.* 1988; Rumsey *et al.* 1990; Gnaiger *et al.* 1995). Up to 30-fold differences in P_{50} reported for mitochondrial respiration continue to separate opposing views on the role of intracellular oxygen in respiratory control and require resolution.

Intracellular oxygen gradients and mitochondrial oxygen kinetics

The study of the oxygen kinetics of isolated cells offers the advantage of observing mitochondrial function largely undisturbed in the intracellular environment (Fig. 2). An experimental example with endothelial cells is shown in Fig. 3. By selecting appropriate cell densities, the transition from kinetic oxygen saturation to anoxia is sufficiently fast to eliminate effects that are unrelated to the regulation of flux by oxygen in the physiological range, without compromising the requirement to obtain a large number of data points during the transition (Fig. 3, inset). Continuous measurement in a closed system offers the advantage of a high density of data points but presents the problem of a non-steady-state process. A quasi-steady state may be realised at each point during a

sufficiently slow transition (Fig. 3), such that externally measured oxygen flux is equal to intracellular diffusional flux and equal to all enzyme-catalysed reaction rates along the respiratory chain (Fig. 1). Hyperbolic oxygen flux/pressure relationships were obtained by non-linear fitting in the oxygen range below 1.1 kPa (Fig. 4; equation 1). The distribution of residuals provides a powerful statistical evaluation (Cornish-Bowden, 1995), both in cells (Fig. 4, inset) and in isolated mitochondria (Gnaiger *et al.* 1995, 1998). In contrast, Petersen *et al.* (1974) show double-reciprocal plots of the oxygen kinetics of isolated rat liver mitochondria in the range below $1 \mu\text{mol l}^{-1} O_2$ (<0.1 kPa), yielding non-linear (non-hyperbolic) patterns in all metabolic states. Their method (P_{50} varies with enzyme concentration; Petersen *et al.* 1976), the narrow oxygen range and the double-reciprocal Lineweaver–Burk plots appear to be inadequate for a statistical test of deviations from a hyperbolic relationship (Cornish-Bowden, 1995).

Interpretation of the oxygen affinity of intact cells is complex owing to the diversity of metabolic states and difficulties in quantification of intracellular oxygen gradients (Jones, 1986; Wittenberg and Wittenberg, 1989; Rumsey *et al.* 1990). Suspended endothelial cells provide a good model for the study of oxygen kinetics because of their small size and regular shape (Fig. 2). Their respiratory rate is 95 % mitochondrial (Steinlechner-Maran *et al.* 1996). The increase in cellular P_{50} with maximum respiratory rate per cell (=oxygen flow, I_{O_2} ; Gnaiger, 1993b) is caused by intracellular oxygen gradients, which increase with oxygen flow, and by a change in mitochondrial P_{50} (Fig. 5). Separation of these interdependent factors is achieved by a comparison of the rate-dependence of P_{50} in identical ranges of oxygen flow in coupled and uncoupled/inhibited cells (Fig. 5). The shallow slope of P_{50} as a function of oxygen-saturated flow, I_{max} , in the

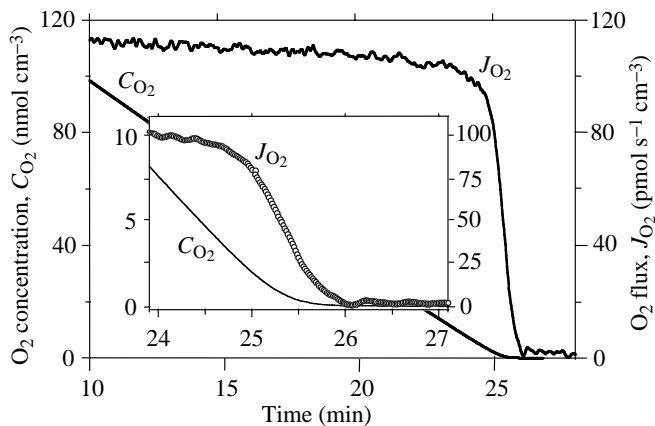


Fig. 3. Experimental records of oxygen concentration, C_{O_2} ($\mu\text{mol l}^{-1} = \text{nmol cm}^{-3}$), and oxygen flux, J_{O_2} ($\text{pmol s}^{-1} \text{cm}^{-3}$), as a function of time. Endothelial cells at a density of $2.9 \times 10^6 \text{ cm}^{-3}$ were studied in the 2 cm^3 closed Oroboros oxygraph chamber (37°C). Inset: low oxygen range ($10 \mu\text{mol l}^{-1} = 1 \text{ kPa}$) and the aerobic–anoxic transition relevant for oxygen kinetics. Each symbol for flux represents one data point.

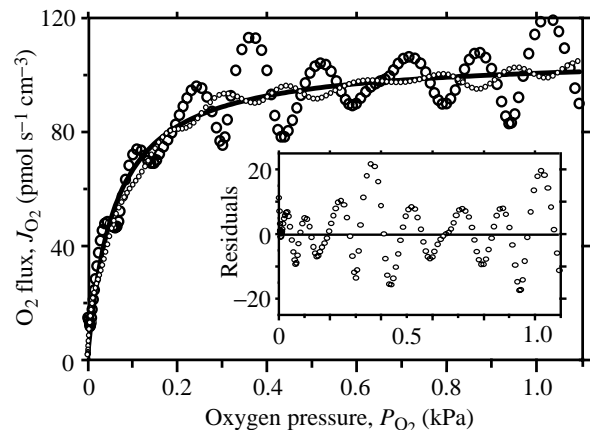


Fig. 4. Oxygen flux, J_{O_2} , plotted as a function of oxygen pressure, P_{O_2} (data from Fig. 2, inset). Solid line, hyperbolic fit ($P_{50} = 0.06 \text{ kPa} = 0.5 \text{ mmHg} = 0.6 \mu\text{mol l}^{-1}$). Large circles, original data; small circles, smoothed data. Oscillations in the original data are instrumental; smoothing shifts the hyperbolic function to the right, with a higher apparent P_{50} . Inset: residuals of the hyperbolic regression, validating the hyperbolic function.

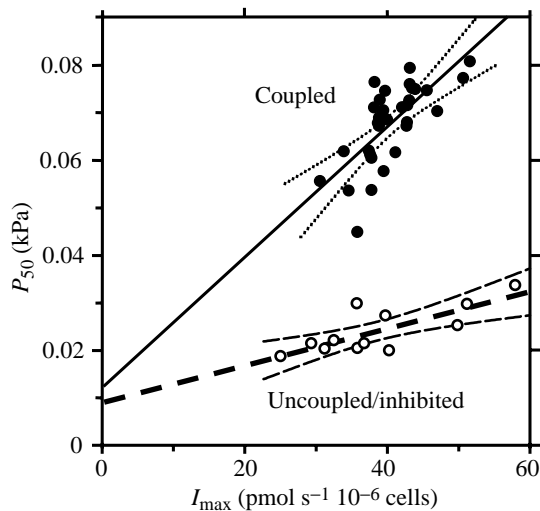


Fig. 5. P_{50} (kPa) as a function of maximum oxygen flow, I_{\max} ($\text{pmol s}^{-1} 10^{-6}$ cells), in endothelial cells in coupled (filled circles, solid line) and in uncoupled/inhibited states ($>4 \mu\text{mol l}^{-1}$ FCCP; open circles, dashed line) in experiments with up to five anoxic exposures (3 min) and partial re-oxygenations. Regression for coupled cells: $y=0.0127+0.00140x$; $r=0.711$, $P<0.0001$; and for uncoupled/inhibited cells: $y=0.0092+0.00039x$; $r=0.773$, $P<0.0032$. 95 % confidence intervals are also shown. Comparison of slopes in an identical range of maximum oxygen flow provides a basis for the separation of the effects of state and rate on P_{50} . A shallow slope for the relationship between P_{50} and oxygen flow indicates a minor influence of intracellular diffusion gradients (modified after Steinlechner-Maran *et al.* 1996).

uncoupled/inhibited state indicates that intracellular oxygen gradients are small. The difference between the slopes of coupled and uncoupled/inhibited cells, therefore, can be interpreted as the diffusion-independent mitochondrial P_{50} (Table 1). The lower P_{50} in uncoupled cells emphasises the importance of metabolic state in the regulation of P_{50} (Steinlechner-Maran *et al.* 1996). A direct test is required with isolated mitochondria.

Fact and artefact

It is becoming increasingly clear that various potential artefacts are confounding factors in mitochondrial oxygen kinetics. These include oxygen gradients in the respirometer, back-diffusion of oxygen from Teflon stirrers, Perspex chambers and inappropriate sealing materials, the low sensitivity of oxygen sensors and insufficient time resolution. These limitations are resolved in high-resolution respirometry, based on the Oroboros oxygraph and DatLab software (Oroboros, Innsbruck, Austria) and on rigorous tests of instrumental background, correction for the exponential time constant of the sensor (3–6 s) and internal calibration of the zero oxygen signal (Gnaiger *et al.* 1995, 1998). The contribution of instrumental artefacts changes with mitochondrial concentration and activation state. Unfortunately, only few studies report adequate methodological tests.

Instrumental background oxygen flux over the experimental oxygen range (Gnaiger *et al.* 1995)

Background measurements yield the change in oxygen concentration over time in the closed system containing incubation medium without biological material. Background oxygen flux results from oxygen consumption by the polarographic oxygen sensor, which is directly proportional to P_{O_2} , and back-diffusion of oxygen into the medium at declining oxygen levels, which is proportional to the P_{O_2} difference between the oxygen source and the medium. Gradual depletion of the oxygen source gives rise to a hysteresis effect. The overall background flux is a near-linear function of oxygen concentration, which is subtracted from the experimental flux at each point of oxygen measurement. A sampling interval of 1 s is appropriate. In addition, occasional microbial contamination is detected by careful background tests.

Independence of P_{50} from concentrations of cells, mitochondria or enzymes at constant metabolic state (Rumsey *et al.* 1990; Steinlechner-Maran *et al.* 1996; Gnaiger *et al.* 1998)

Oxygen flux per volume of the oxygraph chamber, $J_{\text{O}_2, \text{v}}$ ($\text{pmol s}^{-1} \text{cm}^{-3} = \text{nmol l}^{-1} \text{s}^{-1}$), is a function of specific respiratory activity and the concentration of mitochondria, cells or enzyme(s). $J_{\text{O}_2, \text{v}}$ increases proportionally with enzyme concentration. In contrast, P_{50} must be constant, except if (i) concentration exerts an effect on metabolic state (Steinlechner-Maran *et al.* 1996), (ii) the varying aerobic–hypoxic–anoxic transition time influences compensatory processes (Wilson *et al.* 1988) or (iii) different instrumental artefacts are sensitive to different levels of $J_{\text{O}_2, \text{v}}$, particularly the time resolution, the number of data points obtained in the oxygen-dependent region and the ratio of uncorrected background flux to metabolic oxygen flux. We tested our system for concentration effects in the $J_{\text{O}_2, \text{v}}$ range 20–500 $\text{pmol s}^{-1} \text{cm}^{-3}$ at a chamber volume of 2 cm^3 , and observed no significant differences in P_{50} at various mitochondrial dilutions. At higher volume-specific fluxes, erroneously high P_{50} values were obtained (Gnaiger *et al.* 1998; B. Lassnig, A. Kuznetsov, R. Margreiter and E. Gnaiger, in preparation).

Oxygen gradients from a gas–aqueous boundary layer to the oxygen sensor yield low apparent P_{50} values. This artefact might explain the low P_{50} of 0.005 kPa in active skeletal muscle mitochondria at high protein concentration (10 mg cm^{-3} ; Cole *et al.* 1982) in comparison with the value of 0.015 kPa observed on the basis of intracellular myoglobin saturation in resting cardiomyocytes (Wittenberg and Wittenberg, 1985). The latter value agrees closely with the value of 0.025 kPa for skeletal muscle mitochondria determined by high-resolution respirometry (Gnaiger *et al.* 1995) and of 0.008 kPa for passive heart mitochondria (Sugano *et al.* 1974). Although Sugano *et al.* (1974) used a gas–aqueous transfer system, the low mitochondrial density of 0.2 mg cm^{-3} and the spatially dispersed bioluminescence probe reduced the interference by oxygen gradients. A higher P_{50} of 0.04 kPa was obtained for passive heart mitochondria in a closed

Table 1. Mitochondrial P_{50} in passive and active states, with substrates for complexes I or II

| Source | P_{50} (kPa) ^a | | Temperature (°C) | Reference |
|--------------------------------|-----------------------------|--------|------------------|---|
| | Passive | Active | | |
| Heart ^b | 0.008 | 0.08 | 25 | Sugano <i>et al.</i> (1974) |
| | 0.015 ^c | — | 30 | Wittenberg and Wittenberg (1985) |
| | 0.04 | — | 25 | Rumsey <i>et al.</i> (1990) |
| | 0.016 | 0.035 | 30 | B. Lassnig, A. Kuznetsov, R. Margreiter and E. Gnaiger (in preparation); Gnaiger <i>et al.</i> (1998) |
| Liver ^c | 0.06 | — | 25 | Wilson <i>et al.</i> (1988) |
| | 0.025 | — | 25 | Gnaiger <i>et al.</i> (1995) |
| | 0.020 | 0.057 | 30 | B. Lassnig, A. Kuznetsov, R. Margreiter and E. Gnaiger (in preparation); Gnaiger <i>et al.</i> (1998) |
| Endothelial cells ^d | 0.039 | 0.057 | 37 | Steinlechner-Maran <i>et al.</i> (1996) |

^a P_{50} is better expressed in terms of partial pressure (kPa; 1 mmHg=0.133322 kPa) rather than concentration, since oxygen solubility (oxygen concentration per unit partial pressure) decreases with temperature and depends on the composition of the medium. For merely approximate conversion, a solubility of 10 $\mu\text{mol O}_2 \text{ l}^{-1} \text{ kPa}^{-1}$ may be used.

^bIsolated mitochondria, in states 4 (passive) and 3 (active), respiring on substrates for respiratory complex I and II.

^cCardiac myocytes, oxygen partial pressure based on intracellular myoglobin saturation.

^dEndothelial cells, in (not maximally) active and passive states, corrected for intracellular oxygen gradients.

respirometer using a phosphorescence probe (Rumsey *et al.* 1990). The difference may be due to uncorrected oxygen back-diffusion from the Teflon stirrer. Whereas high volume-specific fluxes cause an underestimation of P_{50} due to gradients in steady-state oxygen transfer systems, the opposite effect is produced in closed systems (P_{50} of 0.15 kPa in active heart and liver mitochondria; Costa *et al.* 1997) where fast aerobic–anoxic transitions are beyond the scope of time resolution of the oxygen sensor. In Table 1, results are excluded that appear to suffer from implicit artefacts.

Mitochondrial P_{50} and elasticity in passive and active states

The P_{50} of mitochondrial respiration increases with activation by ADP (Table 1). In heart mitochondria, P_{50} doubles from 0.02 to 0.04 kPa (from 0.12 to 0.26 mmHg), whereas in liver mitochondria P_{50} increases almost threefold from 0.02 to 0.06 kPa (0.43 mmHg) in the active state (B. Lassnig and others, in preparation; Gnaiger *et al.* 1998; Table 1). At an intracellular P_{O_2} of 0.3 kPa, the maximum aerobic performance of heart mitochondria is limited to 90 % of J_{max} (Fig. 6), as derived from equation 1:

$$J_{\text{O}_2} (\% \text{ max}) = \frac{P_{\text{O}_2}}{P_{50} + P_{\text{O}_2}} \times 100. \quad (2)$$

Liver mitochondria would be limited to 84 % of J_{max} at maximum activity (Fig. 6). Insufficient information is available on intracellular P_{O_2} in liver. The relative limitation of flux by a given intracellular oxygen level is equivalent to the elasticity in metabolic control analysis (Fell, 1997):

$$\varepsilon_{\text{O}_2}^J = \frac{P_{50}}{P_{50} + P_{\text{O}_2}}. \quad (3)$$

As shown in Fig. 6, the value of elasticity, $\varepsilon_{\text{O}_2}^J$, is 0.10 in active heart mitochondria and 0.16 in liver mitochondria, and decreases to 0.06 in the passive state. In other words, at intracellular P_{O_2} , mitochondrial flux reaches 94 % of J_{max} in the resting state of zero ATP turnover (Fig. 6). Any evaluation of the physiological role of respiratory control by oxygen must, therefore, take into account tissue-specific differences and the dependence of oxygen affinity on metabolic state and rate. Interpretation of affinities, in turn, is incomplete without simultaneous consideration of maximum flux at each metabolic state.

Catalytic efficiency versus affinity

The decrease in oxygen affinity ($=1/P_{50}$) in active states, when the demand for oxygen is highest, appears to be paradoxical from a functional point of view. While the affinity decreases, however, maximum flux increases greatly, such that the ratio J_{max}/P_{50} is actually increased by adenylate activation (Fig. 7). The scope for activation by ADP declines under hypoxia, but this decline would be even more pronounced at a constant J_{max}/P_{50} ratio (Gnaiger *et al.* 1998). As seen from equation 1, J_{max}/P_{50} is the initial slope of the hyperbolic function:

$$J_{\text{O}_2} = \frac{J_{\text{max}}}{P_{50}} P_{\text{O}_2} \quad (4)$$

when $P_{\text{O}_2} \leq P_{50}$, and reflects the ‘catalytic efficiency’ at low substrate concentrations (Place and Powers, 1984). Apparent catalytic efficiencies can be compared within a system, whereas comparison between different types of mitochondria requires the expression of fluxes in terms of enzyme turnover rates.

Oxygen affinity and catalytic efficiency are highly sensitive

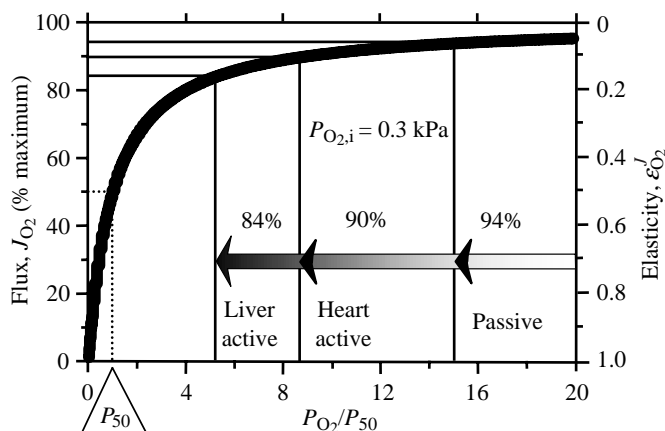


Fig. 6. Oxygen flux J_{O_2} (% of J_{max}) as a function of oxygen pressure P_{O_2} , expressed relative to the P_{50} value for each particular state, and the inverse relationship to the elasticity ϵ'_{O_2} of mitochondrial oxygen flux with respect to oxygen pressure (right-hand y-axis). Arrows indicate the P_{O_2}/P_{50} ratio in the passive and active states in mitochondria isolated from rat heart and liver at an intracellular P_{O_2} of 0.3 kPa. The maximum P_{O_2}/P_{50} ratio of 20 on the x-axis corresponds to the P_{O_2} range below 1.1 kPa in active liver mitochondria. If intracellular P_{O_2} in liver were approximately double that in heart, then active mitochondria would respire at approximately 90 % of maximum capacity in both tissues. Based on equation 2 in the form:

$$J_{O_2} (\% \text{ max}) = \frac{P_{O_2}/P_{50}}{1 + P_{O_2}/P_{50}} \times 100.$$

to uncoupling of oxidative phosphorylation (Fig. 8). At low concentration of carbonyl cyanide *p*-trifluoromethoxyphenylhydrazone (FCCP), uncoupled respiration of endothelial cells increased to a maximum value more than double that for coupled oxygen flow. P_{50} and catalytic efficiency increased concomitantly. Above an optimum uncoupler concentration, oxygen-saturated respiratory flow, I_{max} , declined to the inhibited state, but catalytic efficiency increased further as a function of state and independently of rate (Fig. 8). In the uncoupled/inhibited state (compare Fig. 5), further changes in catalytic efficiency were not significant. Catalytic efficiency increases as thermodynamic efficiency decreases, consistent with a model based on the thermodynamics of irreversible processes (Gnaiger *et al.* 1995). This inverse relationship is not restricted to uncoupling, but also applies to activation by ADP (Fig. 7) when thermodynamic efficiency decreases at maximum power output (Gnaiger, 1993c).

Oxygen affinity and excess capacity of cytochrome *c* oxidase

Threshold effect and flux control coefficient of cytochrome *c* oxidase

ADP and oxygen saturation of mitochondrial respiration at optimum conditions does not drive cytochrome *c* oxidase to

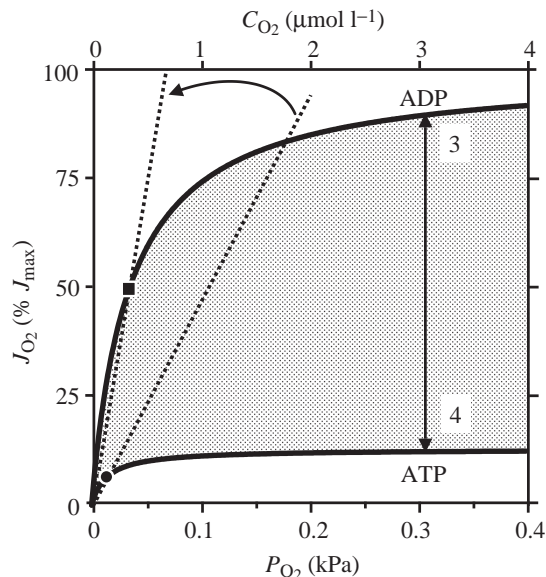


Fig. 7. Oxygen flux, J_{O_2} (as a percentage of J_{max} in the presence of excess ADP), of rat heart mitochondria as a function of oxygen pressure, P_{O_2} (kPa), or oxygen concentration, C_{O_2} ($\mu\text{mol l}^{-1}$), in the passive and active states. The vertical arrow indicates the scope for activation by ADP at an intracellular P_{O_2} of 0.3 kPa (2 mmHg). The circle and square show J_{50} (50% of J_{max}) and P_{50} in states 4 and 3, respectively. The dotted lines through these points show slopes ($0.5J_{max}/P_{50}$), proportional to apparent catalytic efficiency, which increase with activation by ADP (curved arrow). Measurements at 30 °C with pyruvate and malate, and 1 mmol l^{-1} ATP, no ADP (passive, state 4) or 1 mmol l^{-1} ADP plus 1 mmol l^{-1} ATP (active, state 3). 100 % J_{O_2} is equivalent to a state 3 flux of 4.5 nmol $\text{s}^{-1} \text{mg}^{-1}$ mitochondrial protein (from Gnaiger *et al.* 1998).

its kinetic limit: turnover rate can be increased further by the addition of artificial electron donors. COX activity was measured in the oxygraph after blocking complex III with antimycin A (Fig. 1). Reduced *N,N,N',N'*-tetramethyl-*p*-phenylenediamine dihydrochloride (TMPD) served as an electron donor to cytochrome *c*, and its concentration was held constant by the addition of ascorbate. Auto-oxidation of ascorbate and TMPD is a function of oxygen pressure and was subtracted from the measured oxygen consumption as a chemical background (B. Lassnig and others, in preparation). The activity of COX was 50 % and 100 % above maximally ADP-stimulated flux through the respiratory chain in liver and heart mitochondria, respectively, at kinetic oxygen saturation and 500 $\mu\text{mol l}^{-1}$ TMPD (Fig. 9). This is an underestimation since TMPD becomes saturating only at millimolar levels in coupled mitochondria (Morgan and Wikström, 1991).

The phenomenon of an excess capacity of cytochrome *c* oxidase is well known and largely unexplained. The molar ratio between complexes IV and I is six in skeletal muscle (Schwermann *et al.* 1989). COX has a low flux control coefficient, C_{COX}^J , which means that a small change in COX activity plays a minor role in the control of mitochondrial

respiration (Groen *et al.* 1982; using azide for inhibitor titrations). In titrations with cyanide, Kuznetsov *et al.* (1996) found a lower flux control coefficient of COX than with azide. Identical values of maximum fluxes in permeabilized muscle fibres of 50 % COX-deficient mice and controls (Kuznetsov *et al.* 1996) might even suggest a flux control coefficient of zero. The flux control coefficient is the (infinitesimally small) change in relative flux through the pathway over the (infinitesimally small) change in relative capacity of the step (Kacser and Burns, 1973; Heinrich and Rapoport, 1974). High excess capacity is associated with a low flux control coefficient. Correspondingly, C_{COX}^J is increased in muscle fibres of the 50 % COX-deficient mice (Kuznetsov *et al.* 1996). In a theoretical model, C_{COX}^J increases when muscle mitochondria are nearly 50 % oxygen-limited at intracellular oxygen pressure (Korzeniewski and Mazat, 1996), but this lacks support from experimental oxygen kinetics.

A low flux control coefficient is directly related to the threshold effect and explains why COX can be inhibited to a large extent without effect on flux through the respiratory chain (Letellier *et al.* 1993, 1994). The threshold effect of COX may provide a safety margin, protecting against the consequences of accumulations of mutations in mitochondrial DNA (mtDNA) with age (Sohal and Weindruch, 1996) and counteracting genetic defects with mtDNA heteroplasmy, such that a small fraction of wild-type mtDNA remaining in a mitochondrion or cell is sufficient for normal respiratory function (Mazat *et al.* 1997). Importantly, the low flux control coefficient of cytochrome *c* oxidase needs re-evaluation under intracellular P_{O_2} levels (Gnaiger *et al.* 1995).

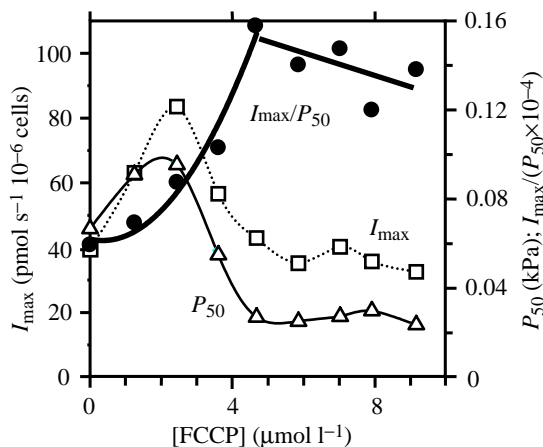


Fig. 8. Maximum oxygen flow, I_{max} , in endothelial cells ($\text{pmol s}^{-1} 10^{-6}$ cells) (open squares) and P_{50} (kPa) (open triangles) as a function of the concentration of the uncoupler FCCP ($\mu\text{mol l}^{-1}$). Maximum stimulation of respiration was observed at FCCP concentrations of 2–3 $\mu\text{mol l}^{-1}$. Higher concentrations caused rapid inhibition of respiration, to I_{max} or below, of coupled cells. Apparent catalytic efficiency, I_{max}/P_{50} (filled circles), increases with uncoupler concentration to a plateau that is reached when respiration is inhibited to a constant minimum value (calculated from data given in Steinlechner-Maran *et al.* 1996).

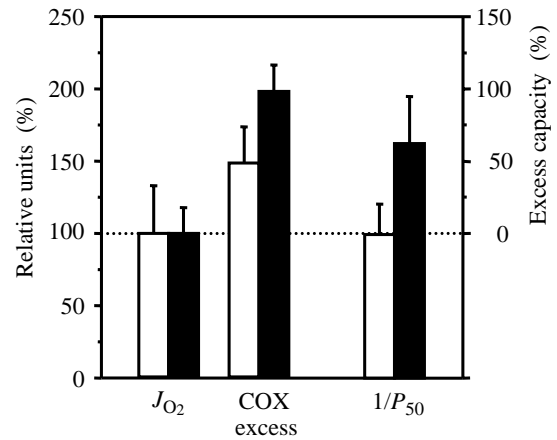


Fig. 9. Excess capacity of cytochrome *c* oxidase (COX) relative to maximum oxygen flux, J_{O_2} , through the respiratory chain and the corresponding oxygen affinity, $1/P_{50}$, in isolated mitochondria from liver (open columns) and heart (filled columns). Fluxes are expressed relative to the respiratory chain (with substrates for complex II in liver, complex I or II in heart). Oxygen affinity is for the active ADP-stimulated state expressed relative to the affinity of liver mitochondria. Error bars show s.d., $N=6-9$. The excess capacity of COX ($500 \mu\text{mol l}^{-1}$ TMPD, 2 or 5 mmol l^{-1} ascorbate, $2.5 \mu\text{mol l}^{-1}$ antimycin A) is significantly higher ($P<0.05$) in heart than in liver mitochondria. The higher excess capacity of COX leads to the higher oxygen affinity of the respiratory chain.

Symmorphosis and flux control analysis

Is the excess capacity of COX non-functional, merely providing a safety margin and expensive insurance against irregular events (Diamond and Hammond, 1992), or does it serve a direct function and is thus compatible with economic design of the respiratory chain? The principle of economic design is well illustrated when considering that the mitochondrial respiratory capacity in skeletal muscle exceeds just slightly the capacity for cardiovascular oxygen supply (Saltin, 1985), and the oxidative capacity of the heart is merely 10–20 % above the maximum physiological performance (Mootha *et al.* 1997). Indeed, the simplest structure–function relationship in the respiratory cascade appears to be at the level of muscle mitochondria, the total volume of which varies in proportion to the aerobic capacity of the organism (Weibel *et al.* 1991). Regardless of allometric variation of body mass and adaptive variation of aerobic scope in athletic *versus* sedentary species, there is a constant relationship of $3.7 \mu\text{mol O}_2 \text{ s}^{-1} \text{ cm}^{-3}$ between the maximum rate of oxygen consumption of the whole organism and mitochondrial volume in the musculature (Hoppeler and Turner, 1989). At a mitochondrial volume of $1.4 \text{ mm}^3 \text{ mg}^{-1}$ mitochondrial protein, this is equivalent to a protein-specific maximum O_2 flux of $4.1 \text{ nmol s}^{-1} \text{ mg}^{-1}$ at 30°C , corresponding to the range of 2–6 $\text{nmol s}^{-1} \text{ mg}^{-1}$ measured in ADP-activated mitochondria isolated from skeletal muscle (Schwerzmann *et al.* 1989) and $4.5 \text{ nmol s}^{-1} \text{ mg}^{-1}$ in active heart mitochondria (Fig. 7). In contrast to the closely matched mitochondrial capacity, there

is excess lung structure in relation to maximum respiration (Weibel *et al.* 1991), suggesting that the flux control coefficient of the lung in the respiratory cascade must be very low under normoxic conditions.

What is the flux control coefficient of mitochondria in the respiratory cascade? Important insights can be derived from our study on mitochondrial oxygen kinetics with the aid of flux control analysis. For this purpose, the respiratory cascade is simplified to three steps (Fig. 1): (1) the lung, with a flux control coefficient of zero; (2) the cardiovascular oxygen supply, including diffusion with a typically high flux control coefficient, C_{supply}^J ; and (3) the mitochondria, with a flux control coefficient, $C_{\text{mito}}^J = 1 - C_{\text{supply}}^J$. Consider a 5% inhibition of mitochondrial capacity in active heart. The competition for oxygen decreases after a reduction in mitochondrial capacity. Consequently, intracellular P_{O_2} tends to increase and flux becomes more oxygen-saturated, relative to a P_{O_2}/P_{50} ratio of approximately 9 (Fig. 6). This pushes J_{O_2} closer to the maximum of the remaining mitochondrial capacity (J_{max} is now 5% less than in the absence of inhibitor; Fig. 6, left-hand y-axis), and a 5% reduction in mitochondrial capacity yields a response of less than 5% in flux; therefore, $C_{\text{mito}}^J < 1$. To compensate fully for any change in flux and to attain $C_{\text{mito}}^J = 0$, intracellular oxygen pressure would have to double to a P_{O_2}/P_{50} ratio of 18, assuming no change in P_{50} . In this new state, the system is driven to a lower elasticity (from 0.1 to 0.05; Fig. 6, right-hand y-axis), and flux is now inevitably more sensitive to a further inhibition of mitochondrial activity, i.e. C_{mito}^J increases as the elasticity decreases. This reflects the well-known connectivity theorem (Kacser and Burns, 1973), application of which shows that a change in elasticity tends to be associated with a change in flux control coefficient in the opposite direction, a very small elasticity corresponds to a large flux control coefficient, and *vice versa*. Elasticity and excess capacity (%) are also related:

$$\text{Excess capacity (\%)} = \frac{P_{50}}{P_{\text{O}_2}} \times 100. \quad (5)$$

At $P_{\text{O}_2} \geq P_{50}$ (on the far right in Fig. 6), the excess capacity is diminishingly small and is equal to the elasticity ($\times 100$; equations 3 and 5).

A mitochondrial excess capacity of 10–20% (Mootha *et al.* 1997) is in line with an elasticity of 0.1 for active heart (Fig. 6). Under these conditions, intracellular oxygen level can be maintained high with respect to mitochondrial P_{50} , but not high enough for full kinetic oxygen saturation of the respiratory chain (Fig. 6). This implies a fairly high mitochondrial flux control coefficient, sharing control with the cardiovascular system. Such distribution of flux control is seen directly in training and in a comparison of sedentary with athletic animals, where the gain in aerobic performance is due to cardiovascular improvement and an accompanying increase in mitochondrial density (Weibel *et al.* 1991).

One central hypothesis of symmorphosis is the matching of capacity for oxygen flux at each step in the respiratory cascade

(Fig. 1) to the maximum flux of the physiological system (Weibel *et al.* 1991). At steady state, oxygen fluxes through each step in the cascade are equal. Does the matching of capacities, therefore, imply that equal capacities of all steps are optimal for economical design? Intuitively, this appears to be the logical implication of symmorphosis. The mechanistic aspects of oxygen kinetics and the mathematical formalism of flux control analysis, however, provide a quantitatively different perspective. Mitochondrial oxidative capacity is conventionally and conveniently measured at kinetic oxygen saturation (Schwerzmann *et al.* 1989; Mootha *et al.* 1997). Full kinetic oxygen saturation would be required, at each mitochondrion in the cell, at a 1:1 matching of the capacities for oxygen consumption and supply. A kinetic saturation of 99% is reached at a P_{O_2}/P_{50} ratio of 100 (equation 2) or at an intracellular P_{O_2} of 3.5 kPa (26 mmHg). Quite apart from the contradiction with experimental observation by a factor of 10, this high intracellular oxygen pressure would seriously reduce the oxygen gradient from haemoglobin to mitochondria and thereby impose additional demands on cardiovascular structure and function to compensate for the lower oxygen pressure head for diffusion. In addition, at a mitochondrial excess capacity of zero, the elasticity reduces to zero and the mitochondrial flux control coefficient is 1, exerting exclusive control over maximum aerobic performance. Equal capacities for mitochondrial oxygen consumption and cardiovascular oxygen supply are not economical.

At the other extreme of an intracellular P_{O_2}/P_{50} ratio of 1 (a factor of 10 below measured P_{O_2} in myocytes), the elasticity for oxygen is increased to 0.5 (Fig. 6). Mitochondrial oxidative capacity would have to be 100% instead of 10% in excess of oxygen supply capacity (equation 5). Such a design is not only uneconomical but impossible, because a doubling of mitochondrial volume density in cardiomyocytes would exceed the available space (Hoppeler *et al.* 1984). Neither zero nor a large mitochondrial excess capacity is economical. Instead, criteria for an optimum excess capacity and optimum distribution of flux control coefficients have to be developed under the constraints set by mitochondrial oxygen kinetics and the intracellular microenvironment (Fig. 6).

Kinetic trapping of oxygen: COX and the respiratory chain

100% excess capacity of mitochondria in the respiratory cascade would present a serious challenge for symmorphosis, and so does the 100% excess capacity of COX in the respiratory chain (Fig. 9). Excess capacities of enzymes in a pathway are required to maintain a catalysed reaction step near equilibrium (for a review, see Suarez, 1996). We propose a new functional explanation of the excess capacity of COX related to the regulation of mitochondrial oxygen affinity, on the basis of (1) the decrease in P_{50} with a reduction in oxygen flux in the transition from the active to the passive state (Fig. 7), (2) the increase in oxygen affinity with an increase in excess capacity of COX in heart *versus* liver (Fig. 9), and (3) a kinetic model of the regulation of the K_m' of cytochrome *c*

oxidase for oxygen (Chance, 1965; Petersen *et al.* 1974; Verkhovsky *et al.* 1996):

$$K_m' = \frac{k_{in}}{k_{et}} K_{eq} \quad (6)$$

K_m' for oxygen of cytochrome *c* oxidase is maintained at a low value by the ratio of rate constants for different reaction steps within the macromolecular structure, where k_{in} is the small, and hence rate-limiting, rate constant for electron input into the enzyme, k_{et} is the excessively large rate constant for the haem-haem electron transfer, and K_{eq} is the equilibrium constant of oxygen binding. A very fast electron transfer to the binuclear haem iron-copper centre of COX corresponds to kinetic trapping of oxygen as a basis for the low K_m' . Variation of k_{et} yields the expected change in the oxygen affinity (Verkhovsky *et al.* 1996). Similarly (Riistama *et al.* 1996):

$$K_m' = \frac{k_{in}}{k_1} K_D \quad (7)$$

where k_1 is the oxygen diffusion rate constant into the binuclear site domain of COX and K_D is the local dissociation constant of the iron-oxygen complex at the reaction centre. Again, restricting the hypothetical oxygen channel into the enzyme, and thus lowering k_1 , effectively increases K_m' of COX (Riistama *et al.* 1996).

In these examples with the isolated enzyme, K_m' of COX is increased by decreasing the 'internal' rate constants, k_{et} or k_1 (equations 6 and 7). In our examples with intact mitochondria, P_{50} of the respiratory chain is decreased by decreasing J_{max} . Since $J_{max} < k_{in}$ (see equation 6), flux control is shifted from the internal rate-limiting electron input into COX to the external electron transport chain, thus reducing COX turnover rate at oxygen saturation. (1) COX turnover rate is reduced at low flux through the respiratory chain in the passive state. This decreases the P_{50} from the active to the passive state. (2) COX turnover rate is reduced at high flux through the respiratory chain by increasing the excess capacity of COX and thus distributing electron input flux to a larger number of enzymes, which yields a lower input rate per enzyme. This decreases the P_{50} in active mitochondria of the heart compared with the liver. Actually, equation 7 provides a similarly plausible model for the functional relationship between the excess capacity of COX and high oxygen affinity. The *integrated* channel area for oxygen diffusion to the reactive centre of COX is enlarged by providing a higher density of COX molecules, which then decreases the P_{50} . This 'synkinetic' regulation of P_{50} depends merely on the quantitative relationship between COX capacity and the respiratory chain, but does not imply kinetic differences between COX in liver and heart (Bonne *et al.* 1993). The apparent excess capacity of COX compared with the aerobic mitochondrial capacity is a basis for the high oxygen affinity of the respiratory chain. It is the necessary price to be paid for the thermodynamic and kinetic optimum function of the respiratory chain within the constraints of oxygen supply through the organismic respiratory cascade and of intracellular oxygen pressure.

This work was supported by a research grant from the University of Innsbruck. A.K. was supported by an Oroburos research award. We thank the Department of Zoology and Limnology, University of Innsbruck (Professor Dr R. Rieger) for the use of the electron microscopy facility. We are grateful for stimulating discussions and cooperation with Professor J.-P. Mazat (Bordeaux).

References

- BABCOCK, G. T. AND WIKSTRÖM, M. (1992). Oxygen activation and the conservation of energy in cell respiration. *Nature* **356**, 301–309.
- BONNE, G., SEIBEL, P., POSSEKEL, S., MARSAC, C. AND KADENBACH, B. (1993). Expression of human cytochrome *c* oxidase subunits during foetal development. *Eur. J. Biochem.* **217**, 1099–1107.
- CHANCE, B. (1965). Reaction of oxygen with the respiratory chain in cells and tissues. *J. gen. Physiol.* **49**, 163–188.
- CHANCE, B., LEIGH, J. S., CLARK, B. J., MARIS, J., KENT, J., NIOKA, S. AND SMITH, D. (1985). Control of oxidative metabolism and oxygen delivery in human skeletal muscle: A steady-state analysis of the work/energy cost transfer function. *Proc. natn. Acad. Sci. U.S.A.* **82**, 8384–8388.
- COLE, R. C., SUKANEK, P. C., WITTENBERG, J. B. AND WITTENBERG, B. A. (1982). Mitochondrial function in the presence of myoglobin. *J. appl. Physiol.* **53**, 1116–1124.
- CORNISH-BOWDEN, A. (1995). *Fundamentals of Enzyme Kinetics*. London: Portland Press.
- COSTA, L. E., MÉNDEZ, G. AND BOVERIS, A. (1997). Oxygen dependence of mitochondrial function measured by high-resolution respirometry in long-term hypoxic rats. *Am. J. Physiol.* **273**, C852–C858.
- DIAMOND, J. AND HAMMOND, K. (1992). The matches, achieved by natural selection, between biological capacities and their natural loads. *Experientia* **48**, 551–557.
- FELL, D. (1997). *Understanding the Control of Metabolism*. London: Portland Press.
- GAYESKI, T. E. J. AND HONIG, C. R. (1991). Intracellular P_{O_2} in individual cardiac myocytes in dogs, cats, rabbits, ferrets and rats. *Am. J. Physiol.* **260**, H522–H531.
- GNAIGER, E. (1993a). Homeostatic and microoxic regulation of respiration in transitions to anaerobic metabolism. In *The Vertebrate Gas Transport Cascade: Adaptations to Environment and Mode of Life* (ed. J. E. P. W. Bicudo), pp. 358–370. Boca Raton, Ann Arbor, London, Tokyo: CRC Press.
- GNAIGER, E. (1993b). Nonequilibrium thermodynamics of energy transformations. *Pure appl. Chem.* **65**, 1983–2002.
- GNAIGER, E. (1993c). Efficiency and power strategies under hypoxia. Is low efficiency at high glycolytic ATP production a paradox? In *Surviving Hypoxia: Mechanisms of Control and Adaptation* (ed. P. W. Hochachka, P. L. Lutz, T. Sick, M. Rosenthal and G. Van den Thillart), pp. 77–109. Boca Raton, Ann Arbor, London, Tokyo: CRC Press.
- GNAIGER, E., LASSNIG, B., KUZNETSOV, A. AND MARGREITER, R. (1998). Mitochondrial respiration in the low oxygen environment of the cell. Effect of ADP on oxygen kinetics. *Biochim. biophys. Acta* (in press).
- GNAIGER, E., STEINLECHNER-MARAN, R., MÉNDEZ, G., EBERL, T. AND MARGREITER, R. (1995). Control of mitochondrial and cellular respiration by oxygen. *J. Bioenerg. Biomembr.* **27**, 583–596.
- GROEN, A. K., WANDERS, R. J. A., WESTERHOFF, H. V., VAN DER

- MEER, R. AND TAGER, J. M. (1982). Quantification of the contribution of various steps to the control of mitochondrial respiration. *J. biol. Chem.* **257**, 2754–2757.
- HEINRICH, R. AND RAPOPORT, T. A. (1974). A linear steady-state treatment of enzymatic chains. General properties, control and effector strength. *Eur. J. Biochem.* **42**, 97–105.
- HELMLINGER, G., YUAN, F., DELLIAN, M. AND JAIN, R. K. (1997). Interstitial pH and PO_2 gradients in solid tumors *in vivo*: High-resolution measurements reveal a lack of correlation. *Nature Medicine* **3**, 177–182.
- HOPPELER, H., LINDSTEDT, S. L., CLAASSEN, J., TAYLOR, C. R., MATHIEOU, O. AND WEIBEL, E. R. (1984). Scaling mitochondrial volume in heart to body mass. *Respir. Physiol.* **55**, 131–137.
- HOPPELER, H. AND TURNER, D. L. (1989). Plasticity of aerobic scope: Adaptation of the respiratory system in animals, organs and cells. In *Energy Transformations in Cells and Organisms* (ed. W. Wieser and E. Gnaiger), pp. 116–122. Stuttgart, New York: Thieme.
- JONES, D. P. (1986). Intracellular diffusion gradients of O_2 and ATP. *Am. J. Physiol.* **250**, C663–C675.
- KACSER, H. AND BURNS, J. A. (1973). The control of flux. *Symp. Soc. exp. Biol.* **32**, 65–104.
- KORZENIEWSKI, B. AND MAZAT, J.-P. (1996). Theoretical studies on control of oxidative phosphorylation in muscle mitochondria at different energy demands and oxygen concentrations. *Acta biotheoretica* **44**, 263–269.
- KUZNETSOV, A., CLARK, J. F., WINKLER, K. AND KUNZ, W. S. (1996). Increase of flux control of cytochrome *c* oxidase in copper-deficient mottled brindled mice. *J. biol. Chem.* **271**, 283–288.
- LETELLIER, T., HEINRICH, R., MALGAT, M. AND MAZAT, J.-P. (1994). The kinetic basis of the threshold effects observed in mitochondrial diseases: a systemic approach. *Biochem. J.* **302**, 171–174.
- LETELLIER, T., MALGAT, M. AND MAZAT, J.-P. (1993). Control of oxidative phosphorylation in rat muscle mitochondria. Implication to mitochondrial myopathies. *Biochim. biophys. Acta* **1141**, 58–64.
- MAZAT, J.-P., LETELLIER, T., BÉDES, F., MALGAT, M., KORZENIEWSKI, B., JOUAVILLE, L. S. AND MORKUNIENE, R. (1997). Metabolic control analysis and threshold effect in oxidative phosphorylation: Implications for mitochondrial pathologies. *Molec. cell. Biochem.* **174**, 143–148.
- MOOTHA, V. K., ARAI, A. E. AND BALABAN, R. S. (1997). Maximum oxidative phosphorylation capacity of the mammalian heart. *Am. J. Physiol.* **272**, H769–H775.
- MORGAN, J. E. AND WIKSTRÖM, M. (1991). Steady-state redox behavior of cytochrome *c*, cytochrome *a* and Cu_A of cytochrome *c* oxidase in intact rat liver mitochondria. *Biochemistry* **1991**, 948–958.
- PETERSEN, L. C., NICHOLLS, P. AND DEGN, H. (1974). The effect of energization on the apparent Michaelis–Menten constant for oxygen in mitochondrial respiration. *Biochem. J.* **142**, 247–252.
- PETERSEN, L. C., NICHOLLS, P. AND DEGN, H. (1976). The effect of oxygen concentration on the steady-state kinetics of the solubilized cytochrome *c* oxidase. *Biochim. biophys. Acta* **452**, 59–65.
- PLACE, A. R. AND POWERS, D. A. (1984). Kinetic characterization of the lactate dehydrogenase (LDH-B₄) allozymes of *Fundulus heteroclitus*. *J. biol. Chem.* **259**, 1309–1318.
- RIISTAMA, S., PUUSTINEN, A., GARCIA-HORSMAN, A., IWATA, S., MICHEL, H. AND WIKSTRÖM, M. (1996). Channelling of dioxygen into the respiratory enzyme. *Biochim. biophys. Acta* **1275**, 1–4.
- RUMSEY, W. L., SCHLOSSER, C., NUUTINEN, E. M., ROBIOLO, M. AND WILSON, D. F. (1990). Cellular energetics and the oxygen dependence of respiration in cardiac myocytes isolated from adult rat. *J. biol. Chem.* **265**, 15392–15402.
- SALTIN, B. (1985). Malleability of the system in overcoming limitations: functional elements. *J. exp. Biol.* **115**, 345–354.
- SCHWERZMANN, K., HOPPELER, H., KAYAR, S. R. AND WEIBEL, E. R. (1989). Oxidative capacity of muscle and mitochondria: Correlation of physiological, biochemical and morphometric characteristics. *Proc. natn. Acad. Sci. U.S.A.* **86**, 1583–1587.
- SOHAL, R. S. AND WEINDRUCH, R. (1996). Oxidative stress, caloric restriction and ageing. *Science* **273**, 59–63.
- STEINLECHNER-MARAN, R., EBERL, T., KUNC, M., MARGREITER, R. AND GNAIGER, E. (1996). Oxygen dependence of respiration in coupled and uncoupled endothelial cells. *Am. J. Physiol.* **271**, C2053–C2061.
- SUAREZ, R. K. (1996). Upper limits to mass-specific metabolic rates. *A. Rev. Physiol.* **58**, 583–605.
- SUGANO, T., OSHINO, N. AND CHANCE, B. (1974). Mitochondrial functions under hypoxic conditions. The steady states of cytochrome *c* reduction and energy metabolism. *Biochim. biophys. Acta* **347**, 340–358.
- TRUMPOWER, B. L. AND GENNIS, R. B. (1994). Energy transduction by cytochrome complexes in mitochondrial and bacterial respiration: The enzymology of coupling electron transfer reactions to transmembrane proton translocation. *A. Rev. Biochem.* **63**, 675–716.
- VERKHOVSKY, M. I., MORGAN, J. E., PUUSTINEN, A. AND WIKSTRÖM, M. (1996). Kinetic trapping of oxygen in cell respiration. *Nature* **380**, 268–270.
- WAGNER, P. D. (1996). Determinants of maximal oxygen transport and utilization. *A. Rev. Physiol.* **58**, 21–50.
- WEIBEL, E. R. (1984). *The Pathway for Oxygen. Structure and Function in the Mammalian Respiratory System*. Cambridge, MA: Harvard University Press. 425pp.
- WEIBEL, E. R., TAYLOR, C. R. AND HOPPELER, H. (1991). The concept of symmorphosis: a testable hypothesis of structure–function relationship. *Proc. natn. Acad. Sci. U.S.A.* **88**, 10357–10361.
- WILSON, D. F., RUMSEY, W. L., GREEN, T. J. AND VANDERKOOI, J. M. (1988). The oxygen dependence of mitochondrial oxidative phosphorylation measured by a new optical method for measuring oxygen concentration. *J. biol. Chem.* **263**, 2712–2718.
- WITTENBERG, B. A. AND WITTENBERG, J. B. (1985). Oxygen pressure gradients in isolated cardiac myocytes. *J. biol. Chem.* **260**, 6548–6554.
- WITTENBERG, B. A. AND WITTENBERG, J. B. (1989). Transport of oxygen in muscle. *A. Rev. Physiol.* **51**, 857–878.